

# An Indirect Adaptive Control Approach to Image Based Visual Servoing for Translational Trajectory Tracking

Jonathan Fried\* Fernando Lizarralde\* Antonio C. Leite\*\*

\* *Dept. of Electrical Eng., Federal University of Rio de Janeiro, Brazil.*

\*\* *Fac. of Sci. and Tech., Norwegian Univ. of Life Sciences, Norway*

---

**Abstract:** In this work, it is considered an image based visual servoing control problem, for uncertain robot manipulators. Visual feedback is provided by a fixed monocular camera with uncertain parameters, for the purpose of tracking translational trajectories of a spherical target, both the trajectory on image plane and depth. Based on a cascade structure, the proposed adaptive visual servoing is combined with an adaptive motion control strategy. Stability and passivity properties are analyzed with the Lyapunov method. Simulation results illustrate and highlight performance of the proposed controller.

*Keywords:* Adaptive Control, Passivity-based control, Tracking, Visual Servoing, Cascade Control

---

## 1. INTRODUCTION

Computer vision is a useful tool to acquire information for robotics, as it mimics human vision and allows for non-contact measurement of the environment. Visual feedback can be provided by single or multiple cameras in a variety of setups, and visual servoing techniques have been broadly studied as a potential tool for medical applications (Krupa et al., 2003), docking of underwater vehicles (Yahya and Arshad, 2016), or exploration and tracking (Zhou et al., 2018), among others.

In this scenario, the uncertainty present in the robot and camera models is a subject of concern since very early development, with a few early adaptive solutions such as (Weiss et al., 1985), where a model reference adaptive controller is used in an image-based visual servoing (IBVS) application for a manipulator with non-negligible, coupled dynamics for planar motion. Interest in adaptive methods for visual servoing is still prominent, for example in UAVs for search-and-rescue missions, self-driving cars or cooperation between multiple manipulators.

In (Wang et al., 2014), an adaptive position-based visual servoing controller for trajectory tracking of nonholonomic mobile robots is proposed, natural image features being used to estimate the position of the robot with visual feedback. In (Leite et al., 2009; Zhang et al., 2019), a hybrid image-based vision/force control is presented, with uncertainty on the parameters for the robot manipulator, camera, and surface constraint. The unknown surface constraints also translate into unknown depth. As the image Jacobian is non-linear for varying depth, the depth is estimated and compensated separately from the Jacobian matrix, similarly to (Wang et al., 2018).

Recently, in (Wang et al., 2018; Leite and Lizarralde, 2016) is considered adaptive visual servoing strategies with separation of the kinematic and dynamic control loops (in the sense of both the design and analysis) without image-space velocity measurements. Both works consider uncalibrated monocular camera and uncertainties in the robot kinematic and dynamic model.

In (Leite and Lizarralde, 2016), a cascade scheme considering passivity properties of each loop is proposed with direct adaptive methods and considering translational motion including target depth control. Using a nonlinear error definition and a linear filter the system stability is guaranteed without using image velocity information. The main drawback of the direct model reference adaptive visual servoing is overparameterization and the limitation on the misalignment angle of the camera frame with respect to the robot base frame.

In (Wang et al., 2018), the separation is obtained proposing a passive/high gain observer with a nonlinear feedback for the kinematic loop. An indirect adaptive image-based planar visual servoing control is proposed to deal with kinematic and camera uncertainties. However, the parameterization and the non explicit cascade of both loops is not straightforward.

This paper proposes an extension of both works (Wang et al., 2018; Leite and Lizarralde, 2016) overcoming their main drawbacks. The translational trajectory tracking problem, considering depth control, is considered using indirect adaptive methods for the kinematic loop, and by means of a passive cascade scheme combining with an adaptive passive control for the dynamic loop. Parameters for both camera and manipulator are considered uncertain with no need of explicit nonlinear feedback and image velocity measurement. To avoid control singularities, a projection mechanism is implemented in the adaptive laws (Cheah et al., 2007).

---

\* This work was financed in part by CNPq/Brazil and the Coordenação de Aperfeiçoamento de Pessoal de Nível Superior - Brasil (CAPES) - Finance Code 001.

## 2. VISUAL SERVOING SYSTEM

A visual servoing setup consists typically of a manipulator and a pinhole camera. In this work, an eye-to-hand setup was used, with a fixed camera tracking a spherical target attached to the manipulator end-effector. In this section, equations for the visual servoing system are presented.

### 2.1 Robot Manipulator Model

Considering a robot manipulator with  $n$  degrees of freedom (DOFs), the end-effector position with respect to the base can be obtained by the forward kinematics given by  $p_b = k(\theta)$ , where  $\theta \in \mathbb{R}^n$  are the joint angles and  $k(\cdot)$  is a vector function. The differential kinematic relates the end-effector linear velocity to joint velocities, given by

$$\dot{p}_b = \frac{\partial k}{\partial \theta} \dot{\theta} = J(\theta) \dot{\theta} \quad (1)$$

where  $J \in \mathbb{R}^{3 \times n}$  is the manipulator Jacobian.

The equation of motion for a  $n$ -DOF manipulator considering an Euler-Lagrange system (Siciliano et al., 2011) is given by:

$$M(\theta) \ddot{\theta} + C(\theta, \dot{\theta}) \dot{\theta} + G(\theta) = \tau \quad (2)$$

where  $M \in \mathbb{R}^{n \times n}$  is the inertia matrix,  $C \in \mathbb{R}^{n \times n}$  are the centripetal/Coriolis forces,  $G \in \mathbb{R}^n$  is a vector of gravitational torques and  $\tau \in \mathbb{R}^n$  is the joint torque vector. This model has the following property:

(P1) The left-hand side of (2) is linearly parameterized with respect to a constant parameter vector  $a_d$ :

$$M(\theta) \ddot{\theta} + C(\theta, \dot{\theta}) \dot{\theta} + G(\theta) = Y_d(\theta, \dot{\theta}, \ddot{\theta}) a_d \quad (3)$$

where  $Y_d(\theta, \dot{\theta}, \ddot{\theta}) \in \mathbb{R}^{n \times d}$  is the regressor matrix, and  $a_d \in \mathbb{R}^d$  is the parameter vector.

Also assume that:

(A1) The lower and upper bounds given by  $\underline{a}_d, \bar{a}_d \in \mathbb{R}$ , respectively, are assumed known and satisfy  $\underline{a}_d \leq \|a_d\| \leq \bar{a}_d$

### 2.2 Visual Servoing Model

Consider the visual tracking problem for an uncertain robot manipulator monitored by a fixed, pinhole camera with uncertain parameters. The control objective is to track a reference trajectory along the  $\{x, y, z\}$  directions.

To accomplish this task, the visual servoing system needs to extract at least three features from a target attached to the manipulator. In this work, a spherical target is considered, so its projection in the image plane is invariant in response to rotations in the 3D environment, making it possible to partially decouple the control of  $x$  and  $y$  from the depth  $z$  (Zachi et al., 2006). The features to be extracted are the centroid of target's projection in the image and the projected area.

Let  $p_c = [x_c \ y_c \ z_c]^T \in \mathbb{R}^3$ , where  $x_c$  and  $y_c$ , in *pixels*, are the coordinates of target centroid expressed in the image frame  $\mathcal{F}_c$ , and  $z_c$ , in  $m$ , is target depth expressed in the camera frame. Let  $p_b = [x_b \ y_b \ z_b]^T \in \mathbb{R}^3$  be the position of

the target, in  $m$ , expressed in the manipulator base frame  $\mathcal{F}_b$ . These two vectors are related by

$$p_c = \begin{bmatrix} \frac{1}{z_c} K_p^\perp \\ K_{p_z} \end{bmatrix} (p_b - p_{bc}) + \begin{bmatrix} O_c \\ 0 \end{bmatrix} \quad (4)$$

where  $K_p^\perp = \begin{bmatrix} f\alpha_x & 0 & 0 \\ 0 & f\alpha_y & 0 \end{bmatrix} R$  and  $K_{p_z} = [0 \ 0 \ 1] R$ ,  $f \in \mathbb{R}$  is the camera focal length in  $mm$ ,  $\alpha_x, \alpha_y \in \mathbb{R}$  are the camera scaling factors in  $pixel/mm$ ,  $R \in SO(3)$  is the rotation matrix between camera and base frame,  $p_{bc}$  is camera position with respect to the base frame and  $O_c$  are the coordinates of the principal point. The differential kinematics that describe the behavior of this system is obtained by directly calculating the derivative of (4) with respect to time:

$$\dot{p}_c = \begin{bmatrix} \frac{1}{z_c} K_p^\perp \\ K_{p_z} \end{bmatrix} \dot{p}_b - \frac{1}{z_c} \begin{bmatrix} p_{xy} & -O_c \\ 0 \end{bmatrix} \dot{z}_c, \quad (5)$$

where  $p_{xy} = [x_c \ y_c]^T$ . Yet, as  $\dot{z}_c = K_{p_z} \dot{p}_b$ ,

$$\dot{p}_c = \begin{bmatrix} \frac{1}{z_c} (K_p^\perp - (p_{xy} - O_c) K_{p_z}) \\ K_{p_z} \end{bmatrix} \dot{p}_b \quad (6)$$

Now, consider depth  $z_c$  and the spherical target of the proposed formulation. Let  $a_c \in \mathbb{R}^+$  be the projected area of the target object in *pixel count*. If so, the relation between those two measurements is given by:

$$(a_c)^{\frac{1}{2}} z_c = \frac{1}{\beta} \quad (7)$$

The following assumptions are considered hereafter:

- (A2) The projected area of the target  $a_c$  is bounded and greater than zero, for all  $t$  in the interval  $[0, \infty)$ ;
- (A3) The sign of  $z_c$  is assumed to be constant and known. Hence, without loss of generality,  $z_c > 0$ , and  $\beta > 0$ ;
- (A4) The effects of radial distortion caused by the camera lens are considered negligible.

The differential kinematics of the depth-to-area transformation is given by deriving (7) with respect to time:

$$\dot{a}_c = -2 \beta (a_c)^{\frac{3}{2}} \dot{z}_c \quad (8)$$

*Complete translational model with area information:* Let  $p_v = [x_c \ y_c \ a_c]^T$  be the vector of image features, expressed in terms of the centroid coordinates and the area of target object. From (6) and (8), the complete visual servoing model is rewritten as follows:

$$\dot{p}_v = \begin{bmatrix} \beta a_c^{\frac{1}{2}} (K_p^\perp - (p_{xy} - O_c) K_{p_z}) \\ -2\beta a_c^{\frac{3}{2}} K_{p_z} \end{bmatrix} \dot{p}_b \quad (9)$$

The differential kinematics for a translational visual servoing system is given by (9) and robot differential kinematic (1), which can be rewritten as:

$$\dot{p}_v = \begin{bmatrix} \beta a_c^{\frac{1}{2}} (J^\perp - (p_{xy} - O_c) J_z) \\ -2\beta a_c^{\frac{3}{2}} J_z \end{bmatrix} \dot{\theta} = J^*(\theta, p_v) \dot{\theta} \quad (10)$$

where  $J^*(\theta, p_v)$  is the feature Jacobian,  $J^\perp = K_p^\perp J$  and  $J_z = K_{p_z} J$  are the image plane and depth Jacobian, respectively. The following property can be stated:

(P2) Consider the image plane Jacobian  $J^\perp$ , the depth Jacobian  $J_z$  and any measurable vector  $\zeta(t)$ , then the following linear parameterization can be established:

$$\beta J^\perp(\theta) \zeta = Y^\perp(\theta, \zeta) a^\perp \quad (11)$$

$$\beta J_z(\theta) \zeta = Y_z(\theta, \zeta) a_z \quad (12)$$

where  $Y^\perp(\theta, \zeta) \in \mathbb{R}^{2 \times p}$  and  $Y_z(\theta, \zeta) \in \mathbb{R}^{1 \times q}$  are the planar and depth kinematic regressor matrices respectively,  $a^\perp \in \mathbb{R}^p$  is a depth-independent parameter vector and  $a_z \in \mathbb{R}^q$  is a constant depth parameter vector.

Let also assume that:

(A5) The lower and upper bound of  $a^\perp$  and  $a_z$  are assumed known and satisfy  $\underline{a}^\perp \leq \|a^\perp\| \leq \bar{a}^\perp$  and  $\underline{a}_z \leq \|a_z\| \leq \bar{a}_z$ .

### 3. ADAPTIVE IBVS FOR TRANSLATIONAL MOTION

In this section, an adaptive visual servoing strategy is proposed for solving the trajectory tracking problem in the presence of an uncalibrated camera and uncertainties in the robot manipulator kinematic and dynamic. Here, the desired trajectory is decoupled in planar and depth trajectories, the former given in terms of the target centroid, the latter in terms of its projected area.

Let  $p_d(t) \in \mathbb{R}^3$  be the desired image features, then the control goal can be described as:

$$p_v(t) \rightarrow p_d(t), \quad e_v(t) = p_v(t) - p_d(t) \rightarrow 0 \quad (13)$$

where  $p_v$  is image feature vector and  $e_v(t) \in \mathbb{R}^3$  represents the image feature error. The following assumptions are made to achieve this goal:

(A6) Translational reference trajectory  $p_d(t)$  remains visible within the robot workspace, and its derivative,  $\dot{p}_d(t)$ , is known and bounded.

(A7) Robot motions are away from singularities.

(A8) Joint angle  $\theta$  and its derivative  $\dot{\theta}$  are measurable.

Thus, it is considered that target occlusion problem does not occur and that inverse of the manipulator Jacobian always exists.

For the visual servoing problem and in order to obtain a separation between a kinematic and dynamic control loop, a cascade control scheme (Leite and Lizarralde, 2016) is used. The dynamic control loop could be solved by the Slotine-Li adaptive scheme, while the kinematic control loop is solved by the indirect adaptive visual servoing.

#### 3.1 Cascade Control

Here, a cascade control scheme is employed (Guenther and Hsu, 1993), choosing a control  $\tau$  which can guarantee a goal  $p_v \rightarrow p_d$  is reached by separating the visual servoing system in kinematic and dynamic control loops. The general strategy is proposed as follows. First, assume that there exists a control law  $\tau = F(\theta, \dot{\theta}, \theta_d, \dot{\theta}_d, \ddot{\theta}_d)$  for (2) which guarantees that  $e(t) = \theta - \theta_d \rightarrow 0$  as  $t \rightarrow \infty$  where  $\theta_d \in \mathbb{R}^n$  denotes the desired trajectory for the dynamic control, assigned to the joint space and assumed uniformly bounded, and  $e$  is the joint position error vector.

Suppose it is possible to define  $\theta_d, \dot{\theta}_d$  and  $\ddot{\theta}_d$  in terms of a control signal  $u$  such that  $u \rightarrow \dot{p}_v$  is given by:

$$\dot{p}_v = J^*(\theta, p_v) [u + \sigma], \quad (14)$$

where  $J^*$  is the feature Jacobian (10) and  $\sigma$  is a vanishing term from the dynamic control yet to be defined.

Therefore, it is possible to design an adaptive visual servoing control law for the kinematic model (14), and considering the cascade structure, to perform the stability analysis for the complete closed loop system.

In the case that the kinematic and dynamic controller could hold passivity properties, the stability analysis is stated by the following theorem:

*Theorem 1.* Consider the following interconnected systems, where  $\Sigma_1$  is the driven system and  $\Sigma_2$  is the driving system, described by:

$$\Sigma_1 : \dot{x}_1 = f_1(x, t) + \xi(x, t)y_2 + \eta(x, t), \quad y_1 = \phi_1(x_1) \quad (15)$$

$$\Sigma_2 : \dot{x}_2 = f_2(x, t) + \omega_2, \quad y_2 = \phi_2(x_2) \quad (16)$$

where  $x = [x_1 \ x_2]^T$ ,  $f_1, f_2$  are piecewise continuous functions in time  $t$  and locally Lipschitz in  $x$  for all  $t > 0$ ;  $x \in \mathcal{D}$ , where  $\mathcal{D} \subset \mathbb{R}^n$  is a domain that contains the origin  $x = 0$ ;  $\phi_1, \phi_2, \xi$  are continuous functions,  $\eta$  is a vanishing perturbation term and  $\omega_2$  is an external input. Suppose that  $\|\eta(x, t)\| \leq \gamma\|x\|$ ,  $\forall t \geq 0, \forall x \in \mathcal{D}$ , where  $\gamma$  is a non-negative constant. Assume that  $\|\xi(x, t)\| \leq c$ ,  $\forall x, t$  and for some  $c > 0$ . If system  $\Sigma_1$  is output strictly passive from  $y_2 \rightarrow y_1$  with positive definite storage function  $V_1(x_1)$

$$\dot{V}_1 \leq -\lambda_1\|y_1\|^2 + c_1\omega_2^T y_1, \quad \lambda_1 > 0 \quad (17)$$

and system  $\Sigma_2$  is output strictly passive from  $\omega_2 \rightarrow y_2$  with positive definite storage function  $V_2(x_2)$

$$\dot{V}_2 \leq -\lambda_2\|y_2\|^2 + c_2\omega_2^T y_2, \quad \lambda_2 > 0. \quad (18)$$

Then, for  $\omega_2 = 0$ , the following properties hold: (i)  $x_1, x_2 \in \mathcal{L}_\infty$  and (ii)  $\lim_{t \rightarrow \infty} y_1(t) = 0$ ,  $\lim_{t \rightarrow \infty} y_2(t) = 0$  (For proof, see Leite and Lizarralde (2016)).

The passivity properties of the proposed adaptive strategy will be explored in the following section using Theorem 1.

#### 3.2 Dynamic Control

Here, we can consider the Slotine-Li adaptive control scheme (Slotine and Li, 1991). This adaptive control has well known passivity properties and it can guarantee that  $\theta(t)$  asymptotically follows a desired trajectory  $\theta_d(t)$ .

Now, consider the virtual error  $\sigma \in \mathbb{R}^n$  defined as:

$$\sigma = \dot{\theta} - \dot{\theta}_r = \dot{e} + \lambda_d e \quad (19)$$

with

$$\dot{\theta}_r = \dot{\theta}_d - \lambda_d e \quad (20)$$

where  $\dot{\theta}_r \in \mathbb{R}^n$  is a velocity reference signal and  $\lambda_d > 0$  is a constant parameter. Now, considering property (P1) (linear parameterization), the following adaptive controller Slotine and Li (1991) can be used:

$$\tau = Y_d(\theta, \dot{\theta}, \ddot{\theta}_r) \hat{a}_d - K_D \sigma + \omega_2, \quad (21)$$

where  $K_d$  is positive definite gain matrix,  $\omega_2 \in \mathbb{R}^n$  is a fictitious external input and  $\hat{a}_d$  is a vector of estimated dynamic parameters, which are updated by

$$\dot{\hat{a}}_d = -\Gamma_d Y_d^T \sigma, \quad \Gamma_d = \Gamma_d^T > 0 \quad (22)$$

where  $\Gamma_d$  is a positive definite gain matrix. Now, defining the parameter error  $\tilde{a}_d = \hat{a}_d - a_d$ , from the robot dynamic

model (3) and the dynamic control law (21), the closed-loop error dynamics is given by

$$M(\theta) \dot{\sigma} + (C(\theta, \dot{\theta}) + K_D) \sigma = Y_d(\theta, \dot{\theta}, \ddot{\theta}_r, \ddot{\theta}_r) \tilde{a}_d + \omega_2 \quad (23)$$

The following theorem establishes passivity properties and stability of this control scheme.

*Theorem 2.* Consider the uncertain robot manipulator dynamic model given by (2), the control law given by (21), the parameterization given by (3) and the parameter adaptation law given by (22). As  $\theta$  and  $\dot{\theta}$  are measurable from assumption (A8), the regressor matrix  $Y_d$  can be calculated. Then, the map  $\omega_2 \rightarrow \sigma$  is output strictly passive with positive definite storage function

$$2V_d = \sigma^T M(\theta) \sigma + \tilde{a}_d^T \Gamma_d^{-1} \tilde{a}_d \quad (24)$$

Moreover, for  $\omega_2 = 0$ , the following properties hold: (i) All system signals are uniformly bounded; (ii)  $\lim_{t \rightarrow \infty} \sigma(t) = 0$ ; (iii)  $\lim_{t \rightarrow \infty} \dot{e}(t) = 0$  and  $\lim_{t \rightarrow \infty} e(t) = 0$  (For proof, see Leite and Lizarralde (2016))

### 3.3 Cascade Strategy

The cascade strategy of the kinematic (10) and dynamic subsystems (23) can now be defined. From (19), one has that  $\dot{\theta} = \dot{\theta}_r + \sigma$ , then the kinematic subsystem can be rewritten as:

$$\dot{p}_v = J^*(\theta, p_v) [\dot{\theta}_r + \sigma] \quad (25)$$

where  $\sigma$  is a vanishing term as stated by Theorem 2. Then a cascade strategy can be proposed considering  $\dot{\theta}_r$  as the visual servoing control signal  $u$ , i.e.  $\dot{\theta}_r = u$ , which define the following visual servoing control system:

$$\dot{p}_v = J^* u + J^* \sigma \quad (26)$$

Note that  $\dot{\theta}_d$  and  $\ddot{\theta}_d$  are now defined in terms of  $u$ :

$$\dot{\theta}_d = u + \lambda_d e, \quad \ddot{\theta}_d = \dot{u} + \lambda_d \dot{e} \quad (27)$$

*Remark 1.* Note that any other passive dynamic control could also be used, for example a variable structure control.

*Remark 2.* Note that control signal  $\tau$  (21) depends on  $\dot{\theta}_r$ . Thus, it is desirable to avoid that  $u = \dot{\theta}_r$  depends directly on  $p_v$ , which would imply on the need of image-space velocity  $\dot{p}_v$  (a very noisy signal). To circumvent this problem, a filtered version of  $p_v$  is used for the design of the visual servoing control signal  $u$ .

### 3.4 Adaptive Kinematic Visual Servoing with Observer

Consider the kinematic visual servoing model given by (26). Then, in order to design a control law  $u$  to solve the visual servoing problem, i.e.  $p_v$  tracking  $p_d(t)$ , linear parameterizations (12) can be considered, consequently the system can be rewritten as

$$\dot{p}_v = \begin{bmatrix} a_c^{\frac{1}{2}} Y^\perp(\theta, u) \\ 0 \end{bmatrix} a^\perp - \begin{bmatrix} a_c^{\frac{1}{2}} (p_{xy} - O_c) \\ 2a_c^{\frac{3}{2}} \end{bmatrix} Y_z(\theta, u) a_z + \omega_1 \quad (28)$$

where  $\omega_1 = J^* \sigma$ .

The idea of using an observer to estimate  $p_{xy}$  in the expression of  $u$  was introduced in (Wang et al., 2018), where it is designed to guarantee the system passivity using a nonlinear feedback term. Here, the proposed observer uses the area information and does not need a

nonlinear feedback term, while still guaranteeing that the kinematic subsystem is output strict passive. Consider  $p_o = [p_{xyo} \ a_c]^T$ , where  $p_{xyo}$  is an estimation of  $p_{xy}$

$$\dot{p}_{xyo} = \underbrace{a_c^{\frac{1}{2}} (\hat{\beta} \hat{J}^\perp - (p_{xy} - O_c + e_{xy}) \hat{\beta} \hat{J}_z)}_{\hat{J}_{xyo}} u - K_o e_o + K_k e_{xy} \quad (29)$$

where  $e_o = p_{xyo} - p_{xy}$  is the observation error,  $e_{xy} = p_{xy} - p_{xyd}$  is the target centroid error and  $K_o \neq K_k > 0$  is a positive gain. Now, rewriting the control law  $u$  is as follows:

$$u = (\hat{J}^*(\theta, p_o))^{-1} [\dot{p}_d - K_k(p_o - p_d)] \quad (30)$$

with

$$\hat{J}^*(\theta, p_o) = \begin{bmatrix} a_c^{\frac{1}{2}} (\hat{\beta} \hat{J}^\perp - (p_{xyo} - O_c) \hat{\beta} \hat{J}_z) \\ -2a_c^{\frac{3}{2}} \hat{\beta} \hat{J}_z \end{bmatrix} \quad (31)$$

note that the structure of  $\hat{J}^*$  is in term of  $p_o$  instead of  $p_v$ , i.e.  $p_{xyo}$  is used instead of  $p_{xy}$ . The parameter adaptation updates are given as follows:

$$\hat{a}^\perp = \Gamma^\perp a_c^{\frac{1}{2}} Y^{\perp T} (e_{xy} - e_o) \quad (32)$$

$$\hat{a}_z = \Gamma_z Y_z^T (a_c^{\frac{1}{2}} e_o^T e_{xy} + a_c^{\frac{1}{2}} (p_{xy} - O_c)^T e_o - \left[ a_c^{\frac{1}{2}} (p_{xy} - O_c) \right]^T e_v) \quad (33)$$

*Projection Algorithm:* To ensure that the inverse of the estimated Jacobian exists in the indirect adaptation, a projection is introduced with the following objectives: (i) avoid the singularity point at the origin; (ii) avoid large parameter drifting. Consider the following projection operator:

$$\Lambda(g, h) = h - \frac{(h^T g) h}{h^T h} \quad (34)$$

Then, the adaptation laws (32) and (33) are modified as:

$$\hat{a}^\perp = \begin{cases} \Lambda(\hat{a}^\perp, \hat{a}^\perp), & \text{for } \|\hat{a}^\perp\| \geq \bar{a}^\perp, \hat{a}^{\perp T} \hat{a}^\perp > 0 \\ \Lambda(\hat{a}^\perp, \hat{a}^\perp), & \text{for } \|\hat{a}^\perp\| \leq \underline{a}^\perp, \hat{a}^{\perp T} \hat{a}^\perp < 0 \\ \hat{a}^\perp, & \text{otherwise.} \end{cases} \quad (35)$$

$$\hat{a}_z = \begin{cases} \Lambda(\hat{a}_z, \hat{a}_z), & \text{for } \|\hat{a}_z\| \geq \bar{a}_z, \hat{a}_z^T \hat{a}_z > 0 \\ \Lambda(\hat{a}_z, \hat{a}_z), & \text{for } \|\hat{a}_z\| \leq \underline{a}_z, \hat{a}_z^T \hat{a}_z < 0 \\ \hat{a}_z, & \text{otherwise.} \end{cases} \quad (36)$$

*Stability Analysis:* Consider the dynamic equation for the tracking error  $e_v$ , and that  $p_{xy} = p_{xyo} - e_o$

$$\dot{e}_v = \begin{bmatrix} \beta a_c^{\frac{1}{2}} (J^\perp - (p_{xyo} - O_c - e_o) J_z) \\ -2\beta a_c^{\frac{3}{2}} J_z \end{bmatrix} u + \omega_1 - \dot{p}_d \quad (37)$$

Now, using the control law (30) and the parameterizations (12), we can obtain the closed-loop error dynamic

$$\dot{e}_v = -K_k e_v - K_k \begin{bmatrix} e_o \\ 0 \end{bmatrix} + a_c^{\frac{1}{2}} \begin{bmatrix} e_o \\ 0 \end{bmatrix} Y_z a_z - \begin{bmatrix} a_c^{\frac{1}{2}} Y^\perp \\ 0 \end{bmatrix} \hat{a}^\perp + \begin{bmatrix} a_c^{\frac{1}{2}} (p_{xy} - O_c) \\ 2a_c^{\frac{3}{2}} \end{bmatrix} Y_z \tilde{a}_z + \omega_1 \quad (38)$$

From (10), (25) and (29) the observation error  $e_o$  dynamic is given by:

$$\begin{aligned} \dot{e}_o = & \hat{J}_{xyo} u - K_o e_o + K_k e_{xy} \\ & - [\beta a_c^{\frac{1}{2}} (J^\perp - (p_{xy} - O_c) J_z)] u - S \omega_1 \end{aligned} \quad (39)$$

where  $S$  is the selection matrix for the first two elements of  $\omega_1$ . Considering the parameterization errors  $\tilde{a}^\perp$  and  $\tilde{a}_z$ , (39) can be rewritten as:

$$\begin{aligned} \dot{e}_o = & -K_o e_o - e_{xy} a_c^{\frac{1}{2}} Y_z \hat{a}_z + K_k (p_{xy} - p_{xyd}) + a_c^{\frac{1}{2}} Y^\perp \tilde{a}^\perp \\ & + a_c^{\frac{1}{2}} (p_{xy} - O_c) Y_z \tilde{a}_z - S \omega_1 \end{aligned} \quad (40)$$

The following theorem shows results on passivity properties and stability analysis of the system.

**Theorem 3.** Consider the uncertain visual servoing problem, modeled by (26), the observer described in (29), the control law given by (30), the parameterizations given by (12), and the parameter adaptation laws given by (32) and (33). Given assumption (A8) ( $\theta$  is measurable), the regressor matrices  $Y^\perp$  and  $Y_z$  can be calculated. Then, given that  $\omega_1 \in \mathcal{L}_2 \cap \mathcal{L}_\infty$ , the map  $\omega_1 \rightarrow e_v - S^T e_o$  is output strictly passive with positive definite storage function

$$2V_{ko} = e_v^T e_v + e_o^T e_o + \tilde{a}^{\perp T} \Gamma^{\perp -1} \tilde{a}^\perp + \tilde{a}_z^T \Gamma_z^{-1} \tilde{a}_z \quad (41)$$

Moreover, for  $\omega_1 = 0$ , the following properties hold: (i) All system signals are uniformly bounded; (ii)  $\lim_{t \rightarrow \infty} e_v(t) = 0$ ; (iii)  $\lim_{t \rightarrow \infty} e_o(t) = 0$ .

**Proof.** The derivative with respect to time of the storage function  $V_k$  (41) is given by

$$\dot{V}_{ko} = e_v^T \dot{e}_v + e_o^T \dot{e}_o + \tilde{a}^{\perp T} \Gamma^{\perp -1} \dot{\tilde{a}}^\perp + \tilde{a}_z^T \Gamma_z^{-1} \dot{\tilde{a}}_z \quad (42)$$

Using the closed-loop error dynamics given by (38) and (40), with the adaptation laws (32) and (33), one has

$$\dot{V}_{ko} = -e_v^T K_k e_v - e_o^T K_o e_o + (e_v^T - e_o^T S) \omega_1 \quad (43)$$

which defines an output strictly passive map, from  $\omega_1 \rightarrow e_v, e_o$ . Thus, if  $\omega_1 = 0$ ,  $\dot{V}_{ko} \leq 0$  which implies, by Lyapunov theory, that  $e_v, e_o, \tilde{a}^\perp$  and  $\tilde{a}_z \in \mathcal{L}_\infty$  and therefore, the equilibrium state is uniformly stable. As  $e_v, e_o, \tilde{a}^\perp$  and  $\tilde{a}_z$  are limited, the derivative with respect to time  $\dot{V}_{ko} = -2e_v^T K_k e_v - 2e_o^T K_o e_o$  is uniformly limited. So, by using the Barbalat's Lemma, it is possible to conclude that  $\lim_{t \rightarrow \infty} e_v(t) \rightarrow 0$  and  $\lim_{t \rightarrow \infty} e_o(t) \rightarrow 0$ . ■

**Remark 3.** Control proposed could be expanded to a redundant manipulator by using the standard generalized inverse of the Jacobian matrix,  $\hat{J}_o^{* \dagger} = \hat{J}_o^{* T} (\hat{J}_o^* \hat{J}_o^{* T})^{-1}$ , in the control law  $u$ .

**Remark 4.** In this work, the target area  $a_c$  is not filtered, and the variation of target area  $\dot{a}_c$  is assumed to be measurable.

**Remark 5.** The separation property of the proposed adaptive kinematic controller allows it to be applied to robots admitting the design of the joint velocity command (e.g., most industrial/commercial robots), provided that joint servoing controller embedded in the system can guarantee that  $\dot{\theta} - u \in L_1 \cap L_\infty$ .

### 3.5 Stability Analysis

Consider now the passivity properties stated by Theorem 2, and of adaptive visual servoing kinematic control system, stated by Theorem 3. Thus, Theorem 1 may be applied to analyze the stability properties of the overall closed-loop cascade system, where the driven system  $\Sigma_1$  and the driving system  $\Sigma_2$  are identified as follows:

$$\Sigma_1 : x_1^T = [e_v^T \ e_o^T \ a^{\perp T} \ a_z^T], \quad y_1 = e_v - S^T e_o \quad (44)$$

$$\Sigma_2 : x_2^T = [e^T \ \dot{e}^T \ a_d^T], \quad y_2 = J^* \sigma, \quad (45)$$

with storage functions  $V_1(x_1) = V_{ko}$  and  $V_2(x_2) = V_d$  as seen in (41) and (24) respectively. Then, from Theorem 1, it is possible to conclude, for the complete adaptive visual servoing system with non-negligible dynamics: (i) All signals of the interconnected system are bounded; (ii)  $\lim_{t \rightarrow \infty} \sigma(t) = 0$ ,  $\lim_{t \rightarrow \infty} e(t) = 0$ ,  $\lim_{t \rightarrow \infty} e_v(t) = 0$ , and  $\lim_{t \rightarrow \infty} e_o(t) = 0$ .

## 4. SIMULATIONS RESULTS

Here, simulations are presented to illustrate the proposed adaptive visual servoing control. Simulations are done with the Matlab/Simulink software. Consider the following visual servoing system:

- A 3R manipulator, with kinematics and dynamics as seen in the simulations of (Leite and Lizarralde, 2016).
- A pinhole camera, where  $f = 8mm$  is its focal length,  $\alpha = 72727pixel/m$  is the camera scaling factor and  $\beta = 0.1$  is the depth-to-area transformation constant. For simplicity, consider that the camera rotation is  $R = R_z(\phi)$ .

The camera transformation mapping, from  $p_b$  to  $p_c$ , is given according to (4) where  $O_c = [0 \ 0]^T$  and  $z_{bc} = 1m$ . The goal  $p_d(t)$  is given by

$$p_d(t) = \begin{bmatrix} 210 + 30 \sin(\frac{\pi}{5}t) + 30 \sin(1.5\frac{\pi}{5}t) \\ -60 + 30 \sin(\frac{\pi}{5}t + 1.6) + 30 \sin(1.5\frac{\pi}{5}t + 1.6) \\ 95 + 3 \sin(0.1t) \end{bmatrix}$$

Regressor matrices  $Y^\perp$ ,  $Y_z$  and  $Y_d$  can be found in (Fried, 2019). Camera misalignment is assumed to be  $\hat{\phi} = \frac{2\pi}{3}$ . Consider the following initial conditions and parameters:  $\theta(0) = [0 \ -\frac{\pi}{4} \ \frac{\pi}{2}]^T$ ,  $\dot{\theta}(0) = 0$ ,  $\hat{a}^\perp(0) = [-5.67 \ -4.35 \ 9.82 \ 7.53]^T$ ,  $\hat{a}_z(0) = [0.027 \ 0.021]^T$ ,  $\hat{a}_d(0) = [0.166 \ 0.302 \ 0.011 \ 0.0114 \ 10.36; 0.4136]^T$ ,  $p_c(0) = [214 \ 0 \ 100]^T$ ,  $p_{oxy}(0) = [210 \ 0]^T$ ,  $K_k = 2\mathcal{I}_3$ ,  $K_o = 4\mathcal{I}_2$ ,  $K_d = 2\mathcal{I}_3$ ,  $\Gamma^\perp = 0.2 \begin{bmatrix} 3 \mathcal{I}_2 & 0 \\ 0 & \mathcal{I}_2 \end{bmatrix}$ ,  $\Gamma_z = 3 \cdot 10^{-6} \begin{bmatrix} 1 & 0 \\ 0 & 2 \end{bmatrix}$ ,  $\Gamma_d = \mathcal{I}_6$ ,  $\bar{a}^\perp = 28.28$ ,  $\underline{a}^\perp = 2$ ,  $\bar{a}^z = 0.13$ ,  $\underline{a}^z = 0.03$ .

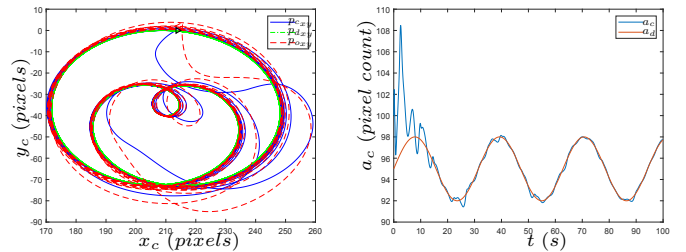


Fig. 1. Dynamic Adaptive IBVS: Image plane Trajectory and Area Tracking

Simulation results are presented in Figures 1-4. The planar trajectory tracking in image space, for both manipulator and observer, and area tracking are presented in Figure

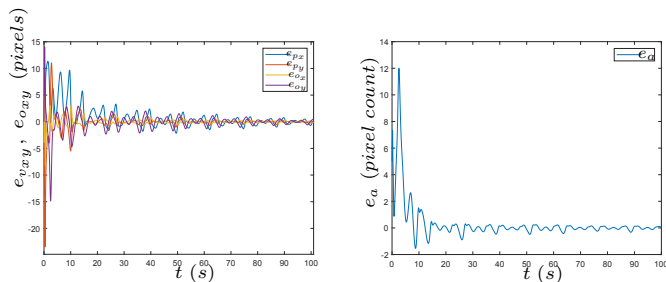


Fig. 2. Dynamic Adaptive IBVS: Image plane, observer and area tracking error

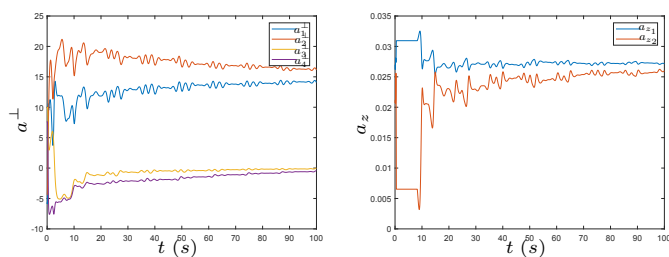


Fig. 3. Dynamic Adaptive IBVS: Depth-independent and Depth-dependent Parameters

1. The error for plane and area trajectory tracking and observer are illustrated in Figure 2. An increasing tracking error is noticeable at the start, due to the initial assumption that  $\hat{\phi} = \frac{2\pi}{3}$ . Figure 3 shows the evolution of estimated parameters  $\hat{a}^\perp$  and  $\hat{a}_z$  over time. The estimated parameters quickly adapt at the start, changing sign near the 1-second mark. Figure 4 shows the control signal, which is visibly bounded, and the dynamic parameters over time. Overall, a feasible control signal and remarkable performance in closed loop were reached, even in the presence of uncertainties in the camera-robot system.

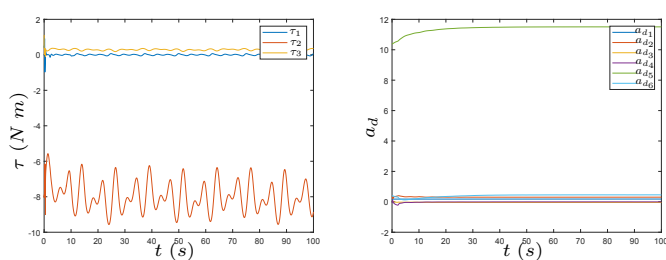


Fig. 4. Dynamic Adaptive IBVS: control signal and dynamic parameters

## 5. CONCLUSION

In this work, the problem of adaptive image based visual servoing is considered for a robot manipulator and eye-to-hand pinhole camera with uncertain parameters for translational trajectory. The idea is to use indirect adaptive methods with a control design to allow planar trajectory and depth tracking simultaneously.

Indirect adaptive schemes for visual servoing does not have the usual restrictions on the camera misalignment,

as presented in direct adaptive control. The simulation shows good performance even for significant uncertainties in camera parameters and misalignment. Future works include developing an observer for the tracked area, study the effects of adaptive schemes in eye-in-hand setups, and considering other image features for tracking, aside from geometric features used in this work.

## REFERENCES

- Cheah, C.C., Liu, C., and Slotine, J.J.E. (2007). Adaptive vision based tracking control of robots with uncertainty in depth information. In *Proc. 2007 IEEE Int. Conf. on Robot. and Autom.*, 2817–2822.
- Fried, J. (2019). *An indirect adaptive Control Approach to Image based Visual Servoing for Translational Trajectory Tracking*. Master’s thesis, Dept. of Elec. Eng., Fed. University of Rio de Janeiro.
- Guenther, R. and Hsu, L. (1993). Variable structure adaptive cascade control of rigid-link electrically-driven robot manipulators. In *Proc. of 32nd IEEE Conf. Decision Contr.*, 2137–2142 vol.3.
- Krupa, A., Gangloff, J., Doignon, C., de Mathelin, M.F., Morel, G., Leroy, J., Soler, L., and Marescaux, J. (2003). Autonomous 3-d positioning of surgical instruments in robotized laparoscopic surgery using visual servoing. *IEEE Trans. Robot. Autom.*, 19(5), 842–853.
- Leite, A., Lizarralde, F., and Hsu, L. (2009). Hybrid adaptive vision-force control for robot manipulators interacting with unknown surfaces. *Int. Journal of Robotics Research*, 28(7), 911–926.
- Leite, A.C. and Lizarralde, F. (2016). Passivity-based adaptive 3d visual servoing without depth and image velocity measurements for uncertain robot manipulators. *Int. J. of Adaptive Contr. and Signal Process.*, 30(8-10), 1269–1297.
- Siciliano, B., Sciacivico, L., Villani, L., and Oriolo, G. (2011). *Robotics: Modeling, Planning and Control*. Springer.
- Slotine, J.J. and Li (1991). *Applied nonlinear control*. Prentice Hall.
- Wang, H., Cheah, C.C., Ren, W., and Xie, Y. (2018). Passive separation approach to adaptive visual tracking for robotic systems. *IEEE Trans. Control Syst. Technol.*, 26(6), 2232–2241.
- Wang, K., Liu, Y., and Li, L. (2014). Visual servoing trajectory tracking of nonholonomic mobile robots without direct position measurement. *IEEE Trans. Robot.*, 30(4), 1026–1035.
- Weiss, L.E., Sanderson, A.C., and Neuman, C.P. (1985). Dynamic visual servo control of robots: An adaptive image-based approach. In *Proc. IEEE Int. Conf. Robot. Autom.*, 662–668.
- Yahya, M.F. and Arshad, M.R. (2016). Position-based visual servoing for underwater docking of an autonomous underwater vehicle. In *IEEE Int. Conf. on Underwater Syst. Technol.*, 121–126.
- Zachi, A.R.L., Liu, H., Lizarralde, F., and Leite, A.C. (2006). Adaptive control of nonlinear visual servoing systems for 3d cartesian tracking. *Controle & Automação (SBA)*, 17, 381 – 390.
- Zhang, Y., Hua, C., and Qian, J. (2019). Adaptive robust visual servoing/force control for robot manipulator with dead-zone input. *IEEE Access*, 7, 129627–129636.
- Zhou, S., Miao, Z., Liu, Z., Zhao, H., Wang, H., Chen, H., and Liu, Y. (2018). Vision-based state estimation and trajectory tracking control of car-like mobile robots with wheel skidding and slipping. In *Proc. of the IEEE/RSJ Int. Conf. on Intellig. Robots&Systems (IROS)*, 4270–4275.